

# BIMS/Filler Interactions. I. Effects of Filler Structure

M. F. Tse

ExxonMobil Chemical Company, Baytown, Texas 77520

Received 26 July 2005; accepted 3 November 2005

DOI 10.1002/app.23789

Published online in Wiley InterScience (www.interscience.wiley.com).

**ABSTRACT:** Polymer/filler interactions have been found to affect the performance of tire tread, sidewall, innerliner, or carcass and other industrial rubber products that are all based on filled elastomers. Identification of types of various polymer/filler interactions and ranking of their impacts have been elusive. Isobutylene-based polymers have relatively saturated structures and contain very low concentrations of functional group. Examples are BIMS (a brominated isobutylene/*p*-methylstyrene copolymer) containing *p*-bromomethylstyrene and *p*-methylstyrene; bromobutyl rubber containing —Br and olefin; chlorobutyl rubber containing —Cl and olefin; and butyl rubber containing olefin. On the other hand, high diene rubbers, such as polybutadiene rubber, polyisoprene rubber, and styrene/butadiene rubber, have unsaturated backbones and high olefin contents.

Hence, different types and extents of interaction with reinforcing fillers, such as carbon black (CB) or silica, are expected in these two classes of elastomer. This work employs bound rubber (solvent extraction), viscoelasticity, stress-strain measurements, and solid state NMR to identify, differentiate, and scale polymer/filler interactions in unvulcanized BIMS/CB, BIMS/silica, SBR/CB, and SBR/silica composites, where SBR denotes a styrene/butadiene rubber. Four different types of CB and one type of silica have been studied. © 2006 Wiley Periodicals, Inc. *J Appl Polym Sci* 100: 4943–4956, 2006

**Key words:** fillers; NMR; rubber; silicas; viscoelastic properties

## INTRODUCTION

A major volume use of rubbers is in tires and mechanical goods, and the rubber compound in service is normally reinforced with filler, such as carbon black (CB) or silica. It is commonly accepted that interactions between polymer and filler will affect rubber compound performance.

Applying complementary viscoelastic and tapping mode atomic force microscopy (AFM) measurements to elucidate the structure–property relationship of CB-filled brominated isobutylene/*p*-methylstyrene copolymer (BIMS) has been reported previously, where the CB is N234 and BIMS denotes a terpolymer of isobutylene, *p*-bromomethylstyrene (BrPMS), and *p*-methylstyrene (PMS).<sup>1</sup> The linear and nonlinear viscoelastic properties of these filled polymers suggest a sharp transition in flow behavior at around 9 vol % filler. The nearest neighbor distances as inferred from AFM measurements also exhibit a sudden change at the same composition. These changes in dynamic and

structural properties were suggested as an indication of the formation of a percolated filler network for composites containing more than 9 vol % CB. With only a few BrPMS groups along a given BIMS chain that are interacting with CB particles, it was proposed that either a single BIMS chain is absorbed onto several filler aggregates or long loops are formed for absorbed chains. The strong mediation of the CB filler network structure by BIMS could be the results of either filler connectivity by BIMS or entanglements of loops from absorbed chains. On the other hand, both rheology and AFM imaging measurements show that the percolation threshold of IMS/N234 is about twice that of BIMS/N234, where IMS denotes an isobutylene/PMS copolymer, the precursor polymer of BIMS.<sup>2</sup> A lower threshold of BIMS/N234 relative to IMS/N234 implies a stronger polymer/filler interaction, which leads to particles with increased effective radius because of the immobilized chains surrounding the particle in the former filled polymer system. Since IMS has no bromine groups, the strong interactions between BIMS and N234 could be attributed to the interactions between the BrPMS groups in BIMS and the surface functional groups on N234. On the other hand, the presence of crosslinking or degradation of BR (polybutadiene rubber) and IR (polyisoprene rubber) at high temperatures during their mixing with N234 or during bound rubber measurements compromises characterization of BR/N234 and IR/N234 interactions.

Part of this paper has been presented at the Rubber Division Meeting, American Chemical Society, Montreal, Quebec, Canada, May 5–8, 1996, and at the Workshop on Interactions of Polymers with Fillers and Nanocomposites, National Institute of Standards and Technology, Gaithersburg, Maryland, June 18, 1998.

Correspondence to: M. F. Tse (mun.f.tse@exxonmobil.com).

Interactions of BIMS and IMS with silica were also studied by bound rubber.<sup>3</sup> Bound rubber increases with increasing vol % silica in the BIMS/silica blend. On the other hand, there is a negligible amount of bound rubber in the IMS/silica blend. Therefore, the strong interactions between BIMS and silica could also be attributed to the interactions between the BrPMS groups in BIMS and the surface functional groups on silica.

## EXPERIMENTAL

### Polymers and fillers

Abbreviations, symbols, and descriptions of the polymers used in this work are shown in Table I. The CB and silica fillers are described in Table II, where DBPA denotes dibutyl phthalate absorption.<sup>4,5</sup> Some polymers and fillers will be discussed in Part II of this study. The contents of BrPMS and PMS in each BIMS polymer were determined from a Varian VXR 300 MHz spectrometer. Molecular weights were measured by gel permeation chromatography, GPC (Waters' Alliance 2690 equipped with UV and DRI detectors), using tetrahydrofuran (THF) as the mobile phase. The description of the two BIMS polymers are shown in Table III and Figure 1. The Mooney viscosity ML (1 + 8) at 125°C was measured according to ASTM D 1646 using radial cavity dies. The SBR used was cold-emulsion polymerized (SBR 1502 from Goodyear Chemical Division), and it had 23.5% bound styrene and 16% vinyl in the butadiene structure. The PiB used was polyisobutylene ( $M_v = 400,000$ ) obtained from Scientific Polymer Products, Inc.

### Mixing and molding

Mixing of the CB stocks (50 phr CB) was carried out in a Banbury internal mixer (started at ~65°C, mixed for ~3–5 min, and discharged at ~150°C), followed by sheeting on a two-roll mill to provide a high level of black dispersion. This mixing and milling process was repeated one more time. On the other hand, mixing of

Filler	Nitrogen surface area (m <sup>2</sup> /g)	DBPA (mL/100 g)
N110 CB	143	113
N234 CB	126	125
N330 CB	83	102
N351 CB	73	120
N660 CB	35	90
N990 CB	6	43
Hi-Sil 233 Silica	150	190

silica-filled stocks (50 phr silica) was carried out in a Brabender mixer (started at room temperature, mixed for ~15–20 min, and discharged at ~98°C), followed by sheeting on a two-roll mill to provide a higher level of silica dispersion. Different mixers were employed to avoid cross-contamination of the black and white compounds. Mixing time of silica in the polymer was longer because silica is more difficult to disperse. No additives other than the fillers were added in these polymer/CB and polymer/silica blends.

Polymers and polymer/filler blends were molded between two pieces of Teflon-coated aluminum foil at 150°C for 25 min. These molded pads (thickness ~2 mm) were then die-cut into appropriate dimensions for viscoelastic and stress–strain measurements. Some polymer/filler blends were molded at 200°C for 20 min. Samples of this kind are termed as “heat-treated”.

### Viscoelastic and stress–strain measurements

Dynamic mechanical experiments were performed using a Rheometrics Dynamic Mechanical Thermal Analyzer (DMTA Mark II). It was operated in bending mode (dual cantilever, flat face/small frame geometry) with a strain of about 0.25%. The sample was a 35.0 × 12.8 mm<sup>2</sup> rectangle with 2-mm thickness die-cut from the molded specimen. All the isochronal (temperature scan) experiments were run at 1 and 10 Hz.

Molded samples were also die-cut into micro-dumbbell specimens having a base of about 1 × 1 cm<sup>2</sup>

TABLE I  
Polymers and Abbreviations

Abbreviation	Description
BIIR	Bromobutyl Rubber
BIMS	Isobutylene/ <i>p</i> -Bromomethylstyrene/ <i>p</i> -Methylstyrene Terpolymer
BR	Polybutadiene Rubber
CIIR	Chlorobutyl Rubber
PiB	Polyisobutylene
IIR	Isobutylene/Isoprene Rubber (Butyl Rubber)
IMS	Isobutylene/ <i>p</i> -Methylstyrene Copolymer
IR	Polyisoprene Rubber
SBR	Styrene/Butadiene Rubber

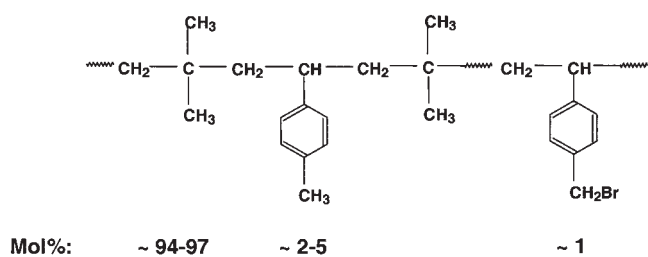


Figure 1 Structure and composition of BIMS polymer.

TABLE III  
Characterization of BIMS Polymers

	BrPMS (mol %)	PMS (mol %)	Mooney at 125°C	Approximate $M_n$	Approximate $M_w$
BIMS 93-4	1.2	2.51	38	170,000	420,000
BIMS 90-10	1.2	2.51	45	190,000	460,000

and the center, narrow strip section of about  $0.6 \times 0.2$  cm<sup>2</sup>. Tensile stress-strain measurements were then performed at different crosshead speeds, and at room temperature and 60°C in an Instron tester. Both the nominal stress, calculated from the undeformed cross-sectional area of the tensile specimen, and the true stress were reported. Strain measurements were based on clamp separation.

### Bound rubber

Procedure for the bound rubber experiment has been described previously.<sup>2</sup> A stainless steel thimble was used to contain the unvulcanized polymer/filler blend for solvent extraction. Bound rubber is the amount of rubber unextractable from the blend after immersion in a solvent, such as cyclohexane, at room temperature for one week. Of course, before the bound rubber

measurements, one wants to make sure that the rubber itself is totally soluble in the solvent. Bound rubber ( $R_B$ ) was then calculated according to the following equation:

$$R_B = \frac{[(\text{Wt. of specimen after immersion} - \text{Wt. of filler in specimen}) \times 100\%]}{(\text{Wt. of polymer in specimen})}$$

Bound rubbers at high temperatures were also measured by extracting the polymer/filler blend with cyclohexane reflux (80°C) and toluene reflux (110°C) for 48 h.

### Synthesis of model compound

*p*-Isopropylbenzyl bromide (PIPBB) was prepared from the corresponding *p*-isopropylbenzyl alcohol

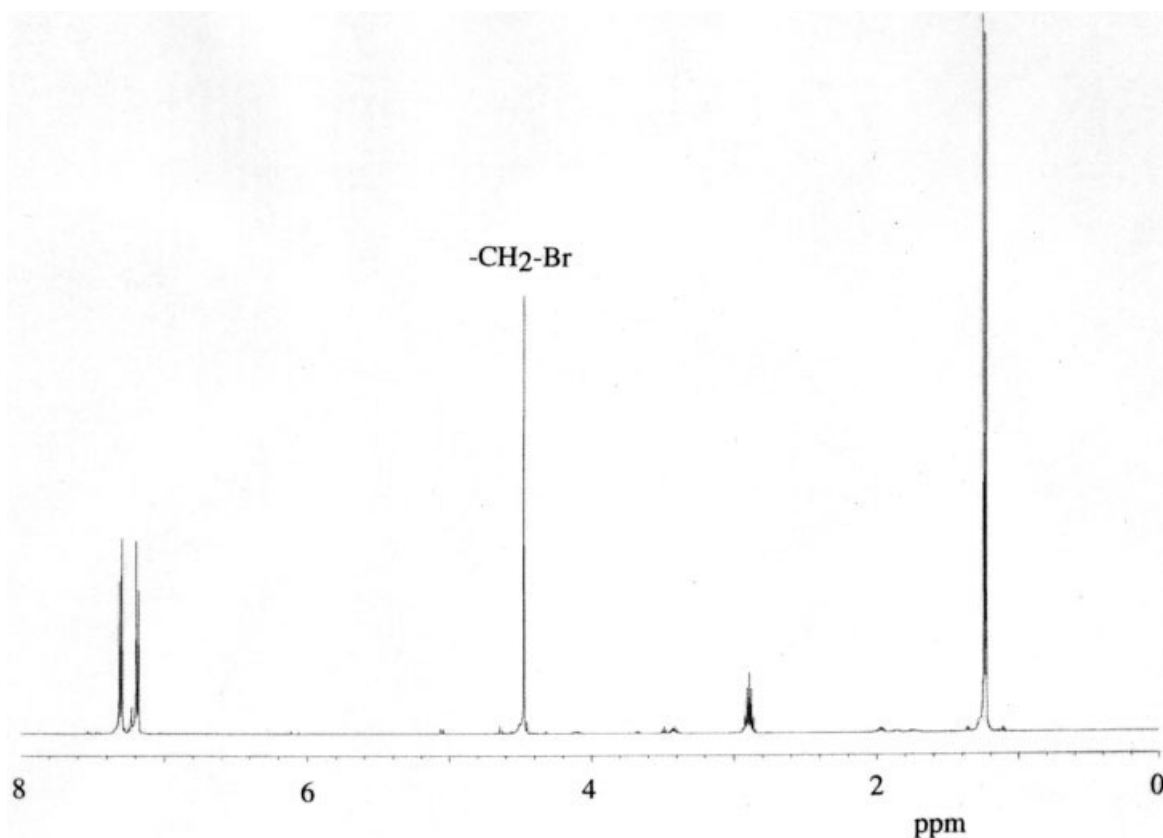
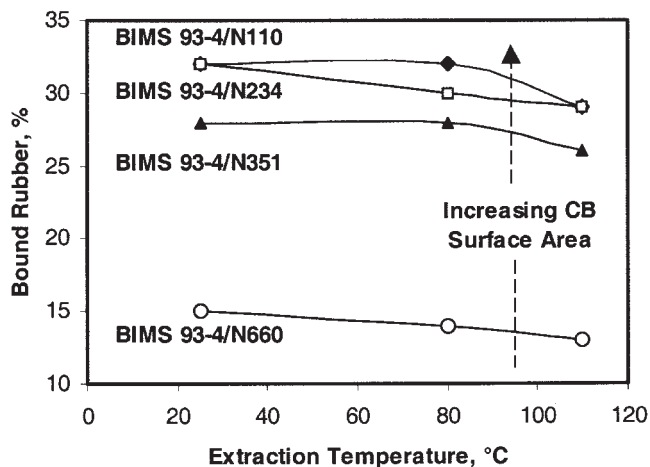
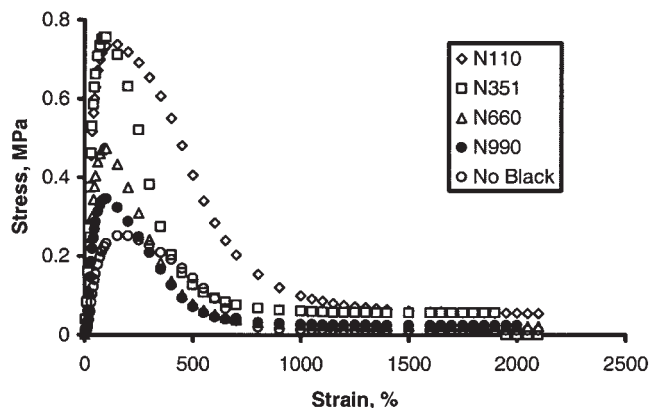


Figure 2 The synthesized compound, PIPBB, shows spectral characteristics consistent with the literature.



**Figure 3** Bound rubber as a function of extraction temperature for BIMS/CB blends.

(PIPBA) and phosphorous tribromide ( $\text{PBr}_3$ ) by a similar procedure used by Bielski et al.<sup>6</sup> The PIPBA (0.15 mol, 22.54 g) was dissolved in 100 mL of THF (anhydrous and inhibitor-free). The solution was cooled in an ice bath for 20 min, and  $\text{PBr}_3$  (0.052 mol, 14.08 g) was added dropwise to avoid fuming (the release of  $\text{HBr}$ ). The mixture, covered by aluminum foil to avoid light exposure, was then stirred at  $0^\circ\text{C}$ . After 2 h, 4 mL of water was added dropwise to destroy the unreacted  $\text{PBr}_3$ . The THF was evaporated and the reaction mixture was a yellowish liquid with some suspending dust (phosphoric acid). This liquid was extracted with 200 mL of chloroform, washed with water for 3–4 times, dried over anhydrous magnesium sulfate, and filtered. An FTIR analysis of this filtered solution revealed the absence of the peak corresponding to PIPBA between  $3300$  and  $3700\text{ cm}^{-1}$ . Finally, the chloroform was evaporated. The PIPBB obtained shows NMR spectral characteristics (Fig. 2) consistent with the literature.<sup>7–8</sup>



**Figure 4** Overall, the larger the surface area of CB, the higher is the yield stress of the BIMS/CB blends in the plot of nominal stress versus strain.

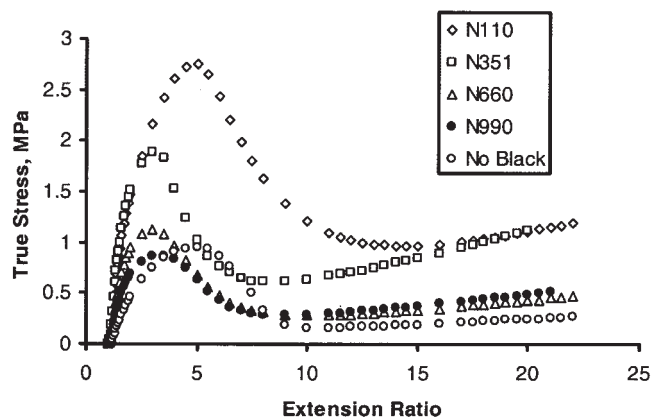


**Figure 5** BIMS and BIMS/CB blends also show yield behavior in the plot of true stress versus extension ratio; extension ratio = 1 + strain.

### Solid state NMR measurements

Two NMR active nuclei,  $^1\text{H}$  (100% natural abundance) and  $^{13}\text{C}$  (1.1% natural abundance), were studied. A Bruker MSL 400 Spectrometer operated at 400 MHz for  $^1\text{H}$  and 100 MHz for  $^{13}\text{C}$  was used to acquire the solid state magic angle spinning (MAS) NMR spectra. The  $\pi/2$  pulses with a recycle delay of 10 s were used. Unfilled and filled polymers were measured at  $150^\circ\text{C}$ , whereas the PIPBB-treated silica was measured at room temperature. The untreated silica was measured both at room temperature and  $150^\circ\text{C}$ .

## RESULTS AND DISCUSSION

### Bound rubber

The interactions of BIMS 93–4 with different types of CB (N110, N234, N351, N660, and N990) were studied. The bound rubber results are shown in Figure 3, where the measurements were performed by solvent extraction at room temperature,  $80^\circ\text{C}$ , and  $110^\circ\text{C}$ . It is clear from Figure 3 that the bound rubber increases

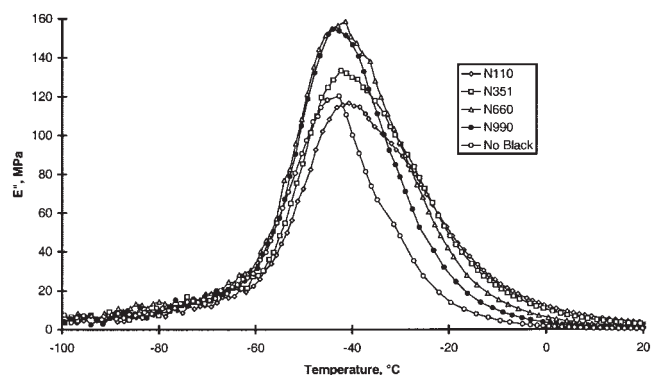


**Figure 6** Overall, the larger the surface area of CB, the broader is the loss modulus peak of the BIMS/CB blends.

TABLE IV  
Coupling Parameter ( $CT_o$ ) of BIMS/CB Blend

	$T_g$ (°C)	$\int E''dT$ (MPa °C)	$w_{1/2}$ (°C)	C	$T_o$ (K)	$CT_o$ (K)	$r^2$
BIMS 93-4/N110	-41	4300	31	0.040	235	9.40	0.978
BIMS 93-4/N351	-42	4700	29	0.039	234	9.13	0.989
BIMS 93-4/N660	-41	5100	26	0.037	231	8.55	0.988
BIMS 93-4/N990	-44	4500	23	0.036	230	8.28	0.994
BIMS 93-4	-43	3300	22	0.035	229	8.02	0.990

with increasing CB specific surface area. However, for each BIMS 93-4/CB blend, the bound rubber does not drop much with increasing extraction temperature. Therefore, N110 and N234 (two tire tread-grade CBs), N351 (a tire sidewall-grade CB), and N660 (a tire innerliner-grade CB) have strong or moderate interactions with BIMS 93-4. The smallest surface-area N990 CB seems to interact weakly with BIMS 93-4 because it leaks out from the metal thimble used in the bound rubber measurements. Therefore, other measurements, such as viscoelastic and stress-strain experiments, were used to characterize BIMS 93-4/N990 interactions described in the next section.

### Stress-strain and viscoelastic properties

The stress-strain curves measured at 25°C and 5.1 cm/min for BIMS 93-4 and four BIMS 93-4/CB blends are shown in Figure 4. Throughout this paper, stress means nominal stress unless otherwise specified. The occurrence of a yield stress in the neat polymer is not understood and this is not a geometrical effect (Fig. 5). A possible explanation is strain-crystallization. After the maximum, the nominal stress in Figure 4 decreases appreciably before the rupture of the specimen. Compared to BIMS, the polymer/filler blends show similar elongations at break, but different yield stresses. Overall, the larger the surface area of the black, the higher is the yield stress of the blend. The enhanced yield stress for the blend containing a larger surface-area CB can be attributed to increased strain amplification (higher bound and/or occluded rubber), re-aggregation of CB particles, improved bonding between polymer and filler, or their combined effects.

The DMTA loss modulus  $E''$  curves as a function of temperature of BIMS 93-4 and the BIMS 93-4/CB blends are shown in Figure 6. The BIMS 93-4/CB blends have broader  $E''$  peaks than the neat BIMS 93-4 polymer. For the blends, the peak width at half height,  $w_{1/2}$ , of the N351 blend is 6°C broader than the N990 blend (Table IV). Stronger polymer/filler interactions introduce more interacting or relaxation species in an amorphous polymeric system. The existence of these

interacting or relaxation species broadens the  $E''$  peak according to the approximate relation shown below<sup>9</sup>:

$$H(\ln\omega) \sim E''(\ln\omega)$$

where  $H(\ln\omega)$  is the distribution of relaxation times and  $\omega$  is the frequency, which is related to the time,  $t$ , by

$$t^{-1} \sim \omega$$

Because of the time-temperature superposition principle,<sup>10</sup> the distribution of relaxation times can also be related to  $E''(T)$ , where  $T$  is the temperature. Therefore, a polymeric system with a broader loss modulus peak will have a broader distribution of relaxation times because of the existence of various relaxing species, which is the result of stronger polymer/filler interactions. Table IV also shows the area under the  $E''(T)$  curve of each BIMS/CB blend compared with the neat BIMS polymer. The filled polymers have quite similar values of  $\int E''dT$ , ranging from 4300 to 5100 MPa °C.

Figure 7 summarizes the widths at half height of the  $E''$  peak and the yield stresses of four of the BIMS 93-4/CB blends as a function of the CB surface area. Overall, larger CB surface areas broaden the  $E''$  peak of the BIMS 93-4/CB blend (equivalent to a broadening in the distribution of relaxation times because of the increased population of various relaxing species).

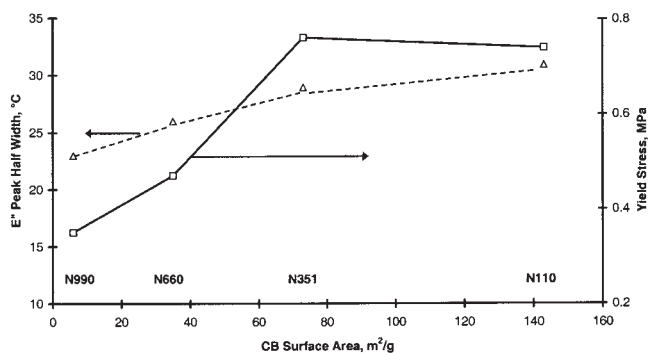
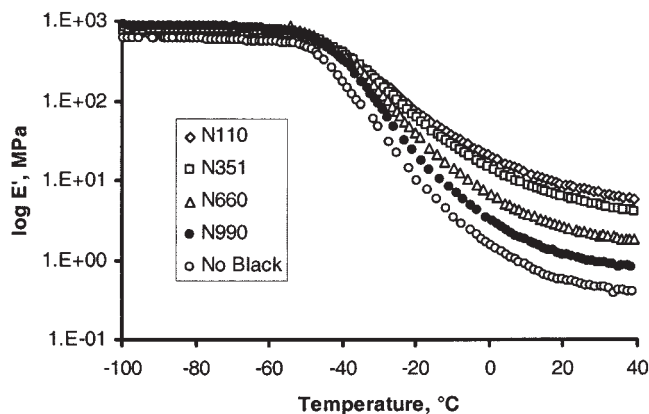


Figure 7 Use of viscoelastic loss modulus peak and tensile yield stress to characterize BIMS/CB interactions.



**Figure 8** The larger surface-area CB introduces a broader or a more gradual drop in  $E'$  (at 10 Hz) of the BIMS/CB blend in the glassy-to-rubbery transition region.

Larger CB surface areas also enhance the yield stress of the blend. According to Figure 3, BIMS blended with a larger surface-area CB has a higher bound rubber. Therefore, a higher bound rubber, a broader  $E''$  peak, and a higher yield stress all suggest stronger BIMS/CB interactions.

The broad  $E''$  peak of the highly interacted polymer/filler blend is also reflected in the behavior of storage modulus  $E'$  of the blend between its glassy-like (local segmental relaxation) and rubber-like (terminal relaxation) regions. This is illustrated in Figure 8, where  $E'$  of the BIMS 93-4/CB system is plotted as a function of temperature. The larger surface-area black will introduce a broader or a more gradual drop in  $E'$  of the polymer/filler blends as the temperature is increased. These  $E'(T)$  data can be expressed by the following sigmoid function:

$$E'(T) - E_r = [E_g - E_r] / \{1 + \exp[(T - T_o)/CT_o]\}$$

or

$$\ln\{[E_g - E'(T)]/[E'(T) - E_r]\} = (T - T_o)/CT_o$$

where  $T$  is the absolute temperature,  $E_g$  the glassy modulus,  $E_r$  the rubbery modulus,  $T_o$  the temperature for  $E'(T)$  at  $[E_g + E_r]/2$ , and  $C$  is a constant. The product  $CT_o$  can be considered as a "coupling parameter," which somehow represents the coupling effects between BIMS and CB to vary  $E'(T)$  between  $E_g$  and  $E_r$ . Note that the  $E_g$  values of the BIMS 93-4/CB blends are quite similar. On the other hand, the  $E_r$  value is higher for the blend containing an CB with a higher surface area. Values of  $C$ ,  $T_o$ , and  $CT_o$  for the various BIMS 93-4/CB blends and the corresponding correlation coefficients  $r^2$  are shown in Table IV, where the  $T_g$  values of the polymer/CB blends were determined from the  $E''$  peak positions and  $w_{1/2}$  is the half

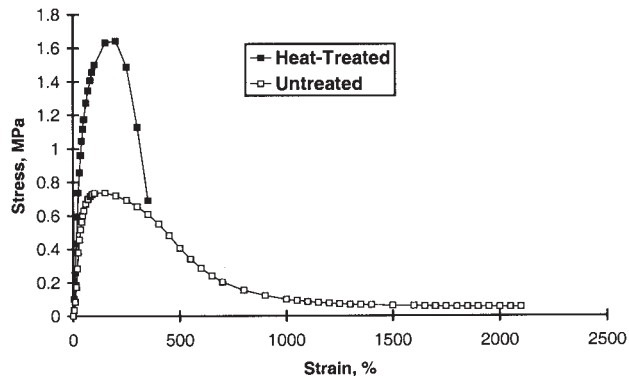
**TABLE V**  
Effects of Heat Treatment on BIMS 93-4 with 50 phr CB

	Bound Rubber ( $R_B$ ; %)		
	25°C	80°C	110°C
BIMS 93-4/N110	32	32	29
BIMS 93-4/N110 (heat-treated)	50	50	48
BIMS 93-4/N351	28	28	26
BIMS 93-4/N351 (heat-treated)	41	41	39
BIMS 93-4/N660	15	14	13
BIMS 93-4/N660 (heat-treated)	25	24	21

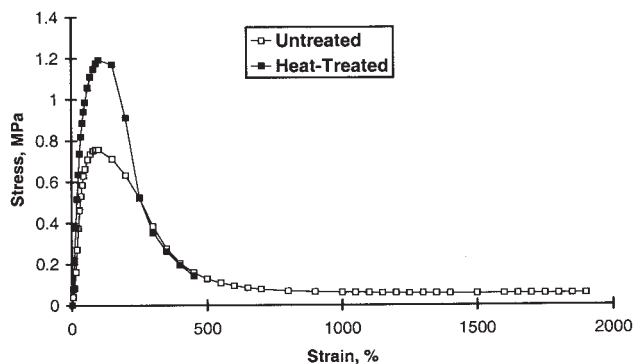
width (peak width at half height) of the  $E''$  peak. The larger the surface area of the black, the larger is the value of  $CT_o$ . Overall, a larger value of  $CT_o$  is equivalent to a more gradual change in the slope of  $E'(T)$  in the neighborhood of  $T = T_o$ . Therefore, besides bound rubber,  $E''$  peak width, and tensile yield stress  $CT_o$  can be used as another representation of polymer/filler interactions, even though there is no significant variation in  $CT_o$  when different types of CB are used.

### Heat treatment

The following discussion compares polymer/filler blends molded at 150°C for 25 min to those (heat-

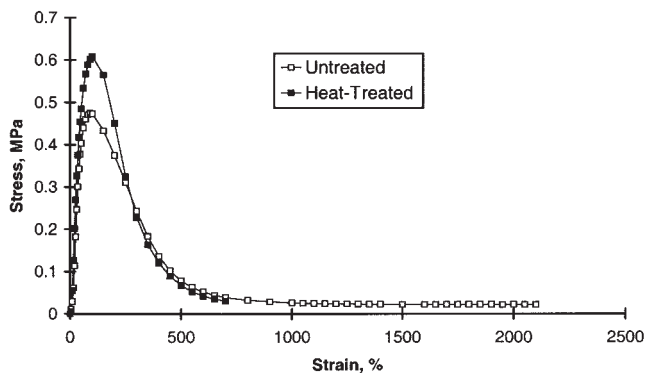


(a)

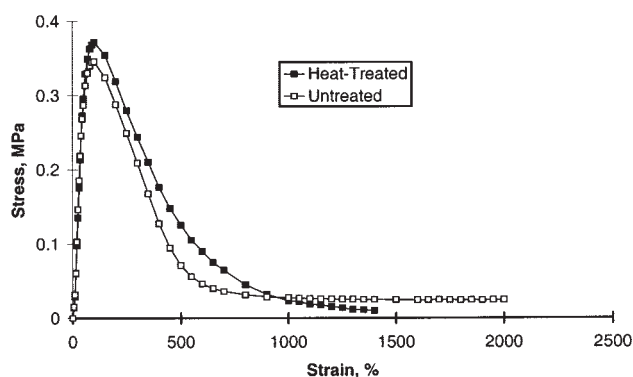


(b)

**Figure 9** The increase in yield stress is more pronounced after the heat treatment for (a) BIMS/N110 and (b) BIMS/N351 blends.



(a)



(b)

**Figure 10** The increase in yield stress is less pronounced after the heat treatment for (a) BIMS/N660 and (b) BIMS/N990 blends.

treated blends) molded at 200°C for 20 min. Gessler<sup>11</sup> heat-treated an IIR/CB compound by a series of alternate heating (160°C for 90 min) and milling (5 min) cycles, and found increases in the tensile moduli and tensile strength, but a decrease in the strain at break of the heat-treated vulcanizate. Similar vulcanizate properties can be obtained by a high temperature Banbury mixing (204–260°C for 10 min). Barton et al.<sup>12</sup> studied

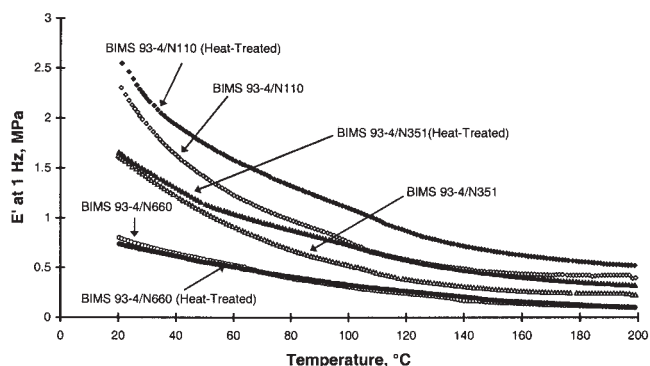


**Figure 11** Heat treatment enhances the high temperature storage modulus of BIMS/CB blends, the effect being more pronounced for the larger surface-area black.

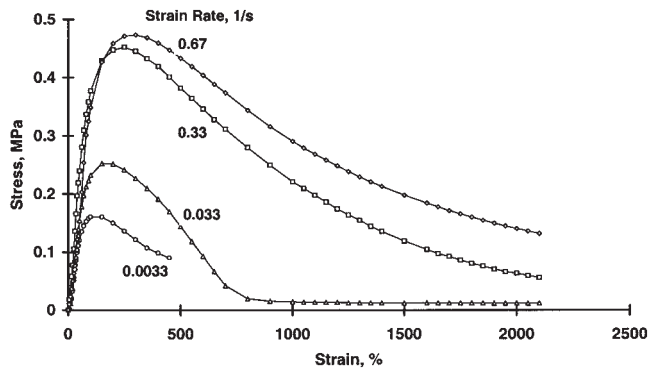


**Figure 12** Strain rate increases the yield stress of the neat BIMS polymer.

the effect of high temperature Banburying on the electrical resistivity of blends of CB with NR, SBR, and IIR's at two levels of unsaturation. They concluded that unsaturation is a necessary prerequisite for the effective heat treatment of polymer/CB blends. Rehner and Gessler<sup>13</sup> indicated that the heat treatment of IIR/CB blends increases the number of polymer/CB bonds through some mechanism involving the isoprene units present in IIR. What we want to show below is the heat treatment of BIMS 93–4/CB blends (no unsaturation in the polymer). Heat treatment of these blends also enhances the bound rubber, the yield stress, and the high temperature storage modulus of the elastomer/CB blends, the effect being more pronounced for CB with a larger surface area.

According to the data in Table V, a molding temperature of 50°C higher raises the bound rubber of some of the BIMS 93–4/CB blends. Heat-treated BIMS/N110 and BIMS/N351 blends not only show higher bound rubbers than their original blends at each extraction temperature, but also exhibit some significant increases in yield stress (Fig. 9). For small surface-area blacks such as N660 and N990, the increase in yield stress after heat treatment is less pronounced (Fig. 10). Consistent with the increases in

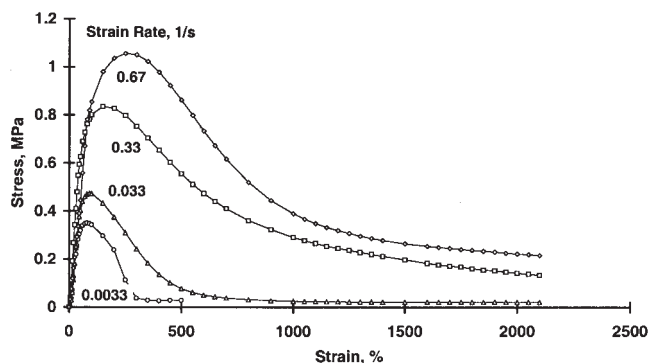


**Figure 13** Strain rate increases the yield stress of the BIMS/N660 blend.

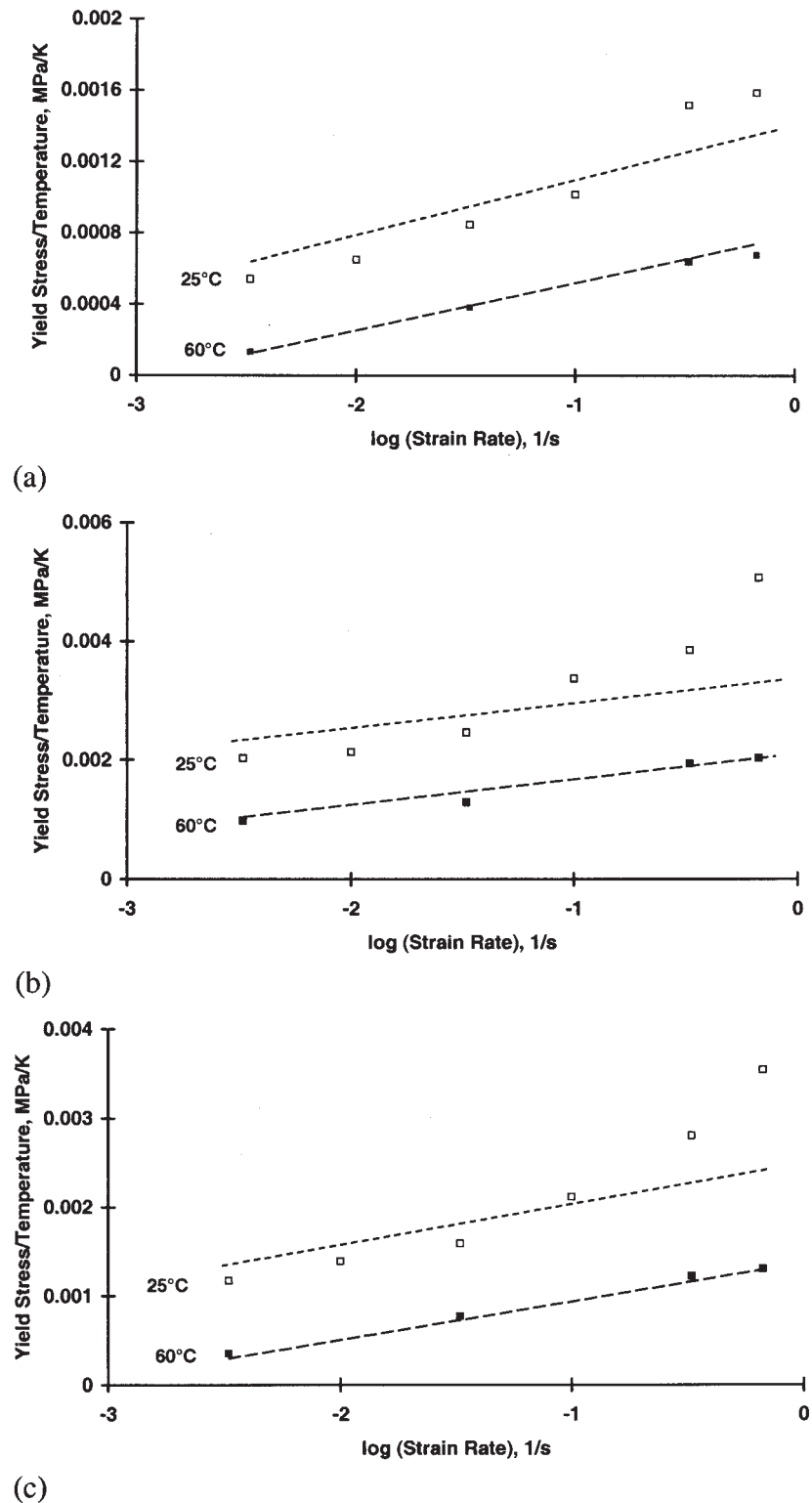


**Figure 14** Yield stress increases with strain rate but decreases with temperature for (a) BIMS, (b) BIMS/N110, and (c) BIMS/N660.

bound rubber and yield stress, heat treatment also enhances the high-temperature storage modulus of the BIMS/CB blend, the effect being more pronounced for the larger surface-area black (Fig. 11). Therefore,

heat treatment of BIMS 93-4 (no unsaturation in the polymer) blended with N110, N351, or N660 results in stronger polymer/filler interactions. Whether the increase in bound rubber of the blend at a higher mold-



ing temperature is due to an improved physical adsorption (van der Waals nature), or an enhanced chemical bonding between the polymer chains and the filler is not clear.

### Flow under a tensile force

The stress-strain behavior of BIMS and BIMS/CB blends at different strain rates and at two temperatures, 25 and 60°C, was studied. Results for BIMS 93-4 and the BIMS 93-4/N660 blend at 25°C are shown in Figures 12 and 13, respectively. In all strain rates, the stress passes through a maximum and then decreases appreciably before the rupture of the specimen. The strain at break of the specimen is drastically reduced when the strain rate goes to the lowest value. With the incorporation of CB, such as N660, in the elastomer, yield stress ( $\sigma_y$ ) is increased at a given strain rate relative to the neat BIMS.

Because the polymer/filler blends are unvulcanized, they flow under the application of a tensile force. Eyring's model provides a basis of analysis of the stress-strain data and the necessary elements for an alternative way to characterize polymer/filler interactions. We attempt to correlate the effects of temperature and strain rate on the flow stress from a molecular model of the flow mechanism. The fundamental concept in the Eyring's model is that a segment of a macromolecule must pass over an energy barrier in moving from one position to another in the polymer. The basic equation for this model is

$$\sigma_y/T = (2/V^*)[(\Delta H/T) + 2.303R\log(\varepsilon/\varepsilon_0)] \quad (1)$$

where  $T$  is the absolute temperature,  $V^*$  is the activation volume (product of the effective area of the polymer segment and the distance from the initial site of the polymer segment to the barrier),  $\Delta H$  is the enthalpy required to take a mole of segments from the potential well to the top of the barrier,  $R$  is the gas constant,  $\varepsilon$  is the strain rate, and  $\varepsilon_0$  is a constant.

Based on eq. (1), we plot  $\sigma_y/T$  versus  $\log \varepsilon$  for BIMS 93-4, BIMS 93-4/N110 blend, and BIMS 93-4/N660

**TABLE VI**  
Flow of BIMS/CB Blend under a Tensile Force

	CB nitrogen surface area (m <sup>2</sup> /g)	V* per Jumping Segment (nm <sup>3</sup> )	$\Delta H$ (kJ/mol)
BIMS 93-4/N110	143	119	120
BIMS 93-4/N351	73	131	118
BIMS 93-4/N660	35	151	109
BIMS 93-4/N990	6	218	101
BIMS 93-4	—	262	91

**TABLE VII**  
High Bound Rubber Corresponds to a Broad Loss Peak, a Higher Yield Stress, but Lower Extension Ratio at Break

	$R_B$ (%)	$w_{1/2}$ (°C)	$T_g$ (°C)	$\sigma_y$ (MPa)	$\lambda_B$
BIMS 90-10	—	20	-44	0.26	>22
BIMS 90-10/N660	12	21	-45	0.65	>22
BIMS 90-10/Silica	75	26	-42	1.35	4
SBR	—	8.0	-39	0.15	13
SBR/N660	14	8.3	-42	0.50	4.5
SBR/Silica	28	16	-38	3.08	1.5

blend in Figure 14. From these we can determine  $V^*$  and  $\Delta H$ , and the results for all the other systems are shown in Table VI. Overall, the larger the CB surface area, the smaller is the  $V^*$  per jumping segment and the higher is the  $\Delta H$ . Therefore, both  $V^*$  and  $\Delta H$  can be used to scale polymer/filler interactions qualitatively.

### Polymer/CB and polymer/silica blends

Bound rubber results of BIMS 90-10/filler blends compared with SBR/filler blends are shown in Table VII. These blends are unvulcanized and contain 50 phr filler. BIMS has a higher amount of bound rubber with silica compared with SBR. However, the bound rubber of BIMS with N660 is comparable to that of SBR with the same filler. Therefore, it appears that BrPMS in BIMS has stronger interactions with silica compared to the unsaturation in SBR. On the other hand, they have similar degrees of interaction with N660. Whether the interactions are physical or chemical in origin, or a combination of both types, will be discussed in subsequent sections.

Figures 15 and 16 show the loss modulus curves as a function of temperature for the BIMS/filler and SBR/filler systems, respectively. Both silica-filled BIMS and SBR polymers have broader loss modulus

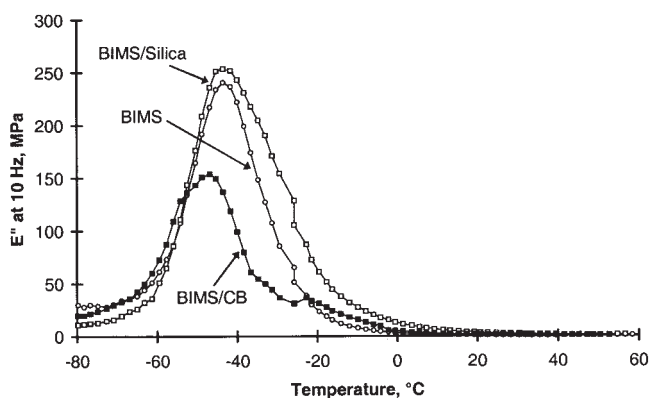


**Figure 15** BIMS/silica shows a broader loss modulus peak than BIMS/N660.

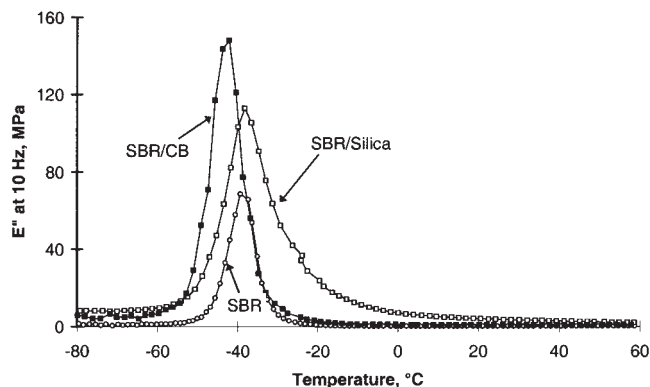


**Figure 16** SBR/silica shows a broader loss modulus peak than SBR/N660.

peaks than the corresponding N660-filled BIMS and SBR counterparts. The width of the loss peak is characterized by  $w_{1/2}$  (Table VII). Similar to that discussed before, for a given polymer, the polymer/filler system with a higher bound rubber also has a broader loss peak (or a broader distribution of relaxation times). It is more likely that the filler surface modifies the polymer matrix in a way that physical properties of the polymer will change continuously with increasing distance from the filler surface. The result should be a broadening in the measured transition region and a slight change in the average  $T_g$  of the composite. At least, part of the broadening of the transition region is due to the heterogeneity in the molecular weight of the original polymer chain introduced by polymer/filler attachment points.

Figures 17 and 18 show the stress–strain curves of BIMS/CB, BIMS/silica, SBR/CB, and SBR/silica compared with their unfilled polymers. If CB is incorporated into BIMS, the maximum stress is raised and the strain at break remains the same as the unfilled BIMS. On the other hand, if silica is incorporated into BIMS, the maximum stress is raised even higher with a substantial reduction in the strain at break. A similar

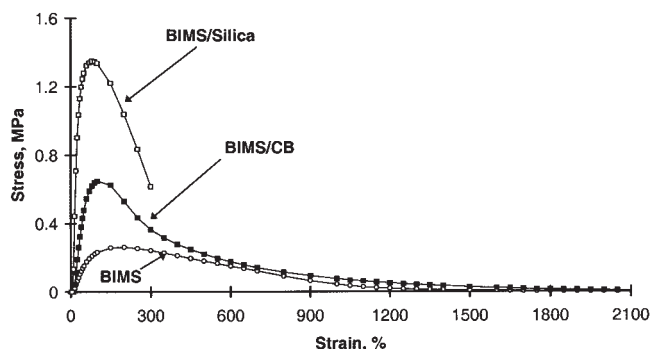


**Figure 17** Overall, filler increases the yield stress but decreases the strain at break of BIMS (test temperature = 25°C; strain rate = 2.2 min<sup>-1</sup>).

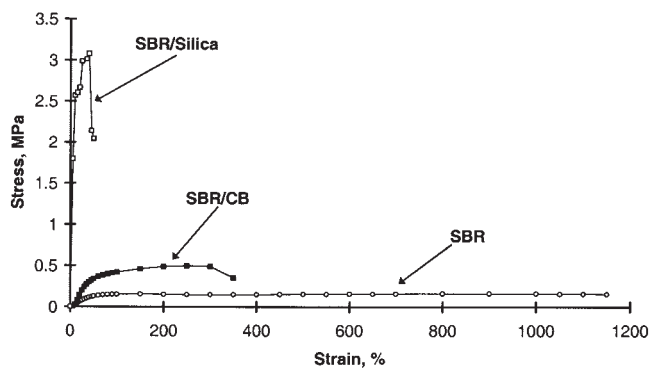


**Figure 18** Overall, filler increases the yield stress but decreases the strain at break of SBR (test temperature = 25°C; strain rate = 2.2 min<sup>-1</sup>).

conclusion can be applied to the stress–strain curves of SBR/CB and SBR/silica compared with that of SBR Fig. 18. Table VII summarizes the above results. It suggests that a stronger polymer/filler interaction, as indicated by a higher  $R_B$ , corresponds to a higher  $\sigma_y$  and a bigger drop in  $\lambda_B$  for a given polymeric system, where  $\lambda_B$  is the extension ratio at break, defined as (1 + strain at break).

### Solid state NMR of BIMS/silica blends

Solid state MAS <sup>1</sup>H NMR has been employed to investigate the type of interaction between BIMS 90–10 and silica. Figure 19 shows results measured at 150°C for BIMS and BIMS/silica. Assignments of some important peaks are shown. BIMS does not appear to react chemically with silica because there is no detectable change in shift or intensity of the peak associated with the BrPMS group at ~4.4 ppm. However, this peak is broadened after the incorporation of silica in BIMS [Fig. 19(b)]. Then, two questions arise: (1) is there any association (e.g.: hydrogen bonding) existing between the ≡Si—OH group on silica and the BrPMS group in BIMS, and (2) is there any interaction between the ≡Si—OH group on silica and the PMS group in BIMS?

Proton solid state NMR measurements of the silica, the blend of an unbrominated BIMS (IMS) with 50 phr silica, and the blend of a PiB with 50 phr silica were carried out to answer these questions. The IMS has PMS groups, but no BrPMS functionality. On the other hand, PiB has no PMS and BrPMS groups.

Figure 20 shows the <sup>1</sup>H NMR spectra of silica measured at room temperature and 150°C. Interestingly, the silanol hydrogens appear also at ~4.4 ppm. The peak at ≥10 ppm is due to water adsorbed on silica because its intensity drops significantly when the sample is run at 150°C.

Figure 21 shows the <sup>1</sup>H NMR spectra of IMS/silica and PiB/silica blends. On the basis of Figure 20 (NMR

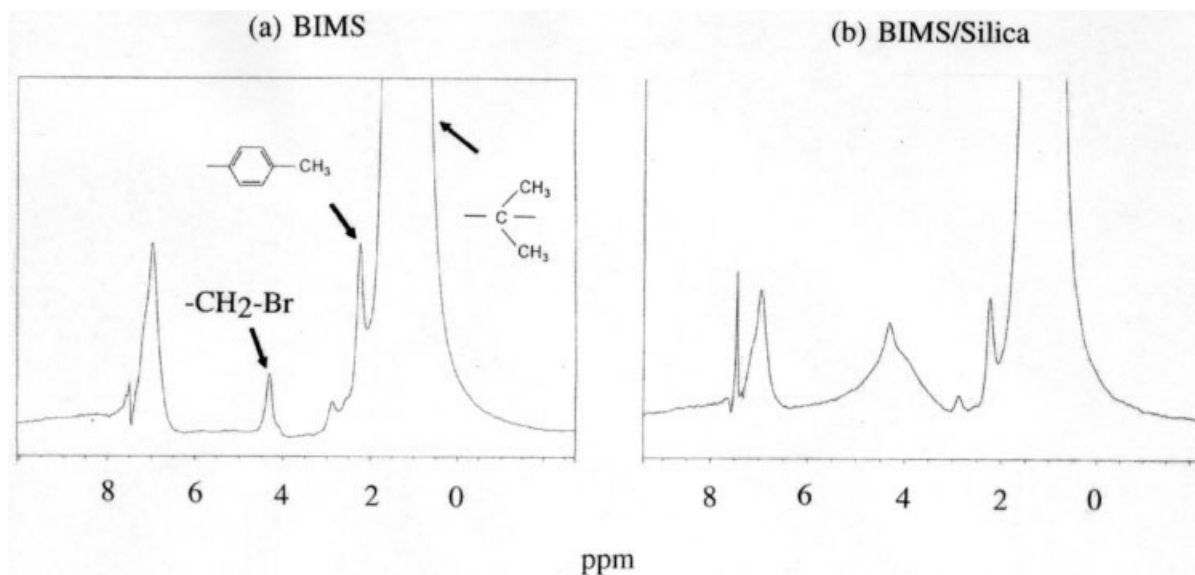


**Figure 19** The incorporation of silica in BIMS does not shift the peak associated with the BrPMS group; however, a broadening of this peak occurs.

spectra of silica), the broadening in the peak associated with the BrPMS group in BIMS/silica [Fig. 19(b)] is due to superposition of the peak associated with the silanol group,  $\equiv\text{Si}-\text{OH}$ , on silica. Similarly, the  $\equiv\text{Si}-\text{OH}$  peak of the PiB/silica blend also occurs at

$\sim 4.4$  ppm [Fig. 21(b)]. This provides indirect evidence that the BrPMS group and the PMS group in BIMS do not affect the electronic environment of the proton in the  $\equiv\text{Si}-\text{OH}$  group on silica. Therefore, any association is unlikely to happen.

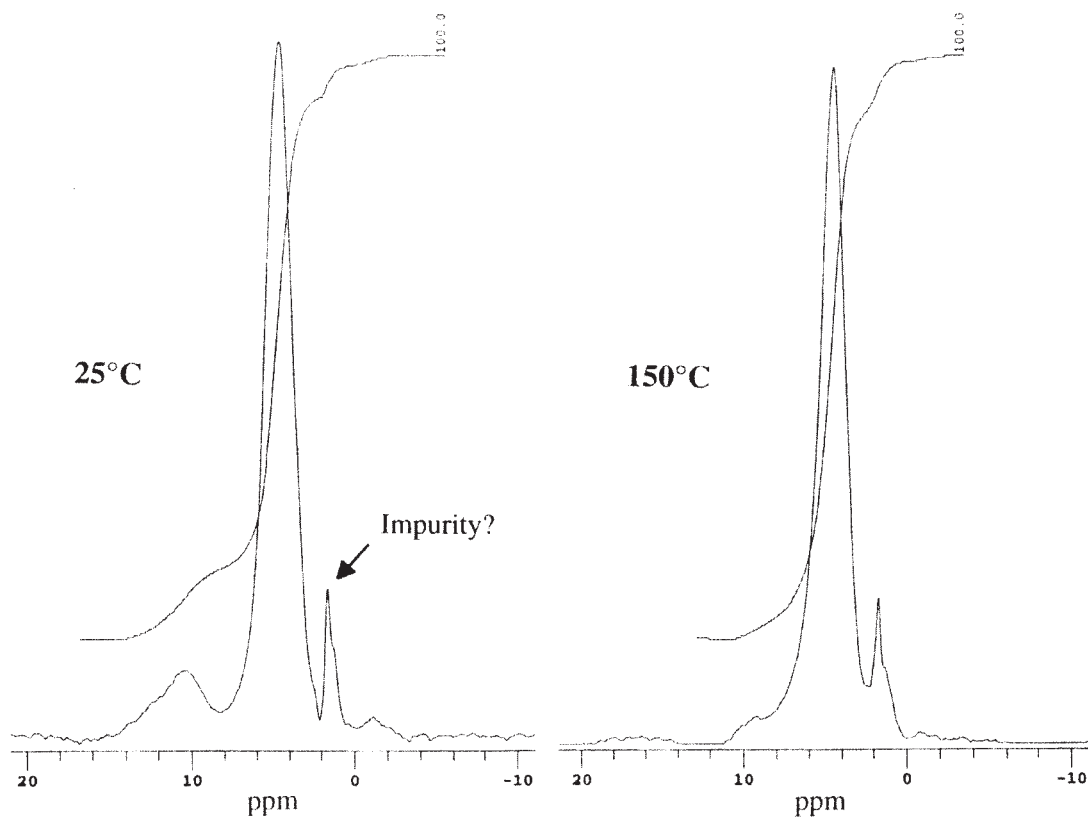


**Figure 20** The  $^1\text{H}$  NMR spectra of silica measured at room temperature and 150°C.

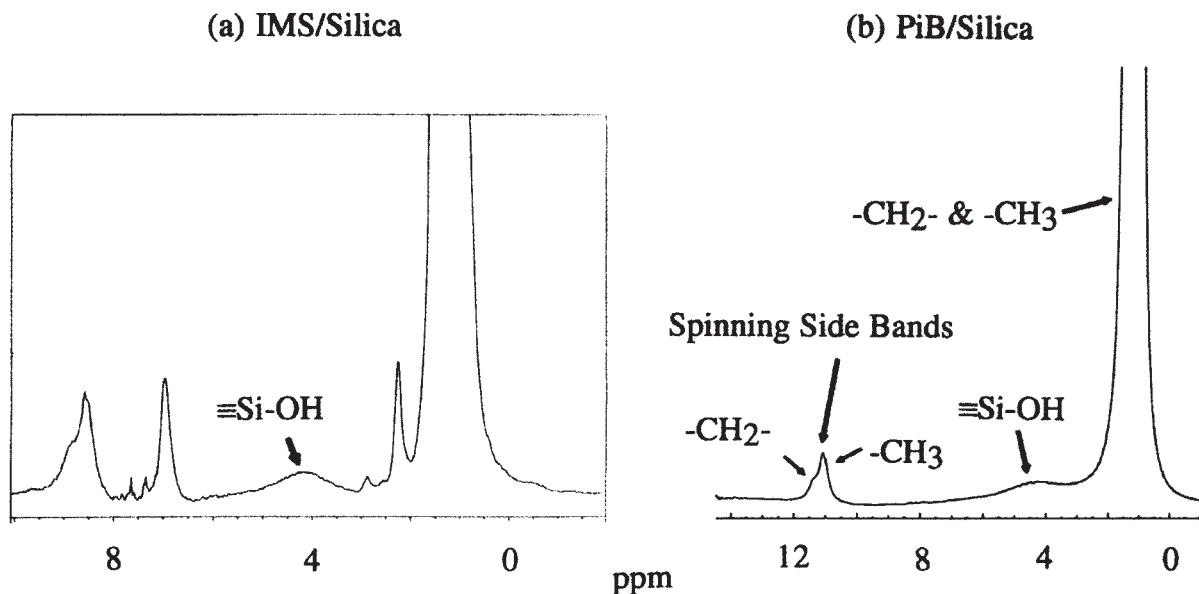


Figure 21 The effect of silica on the  $^1\text{H}$  solid state NMR spectra of IMS and PiB.

To gain further insight into BIMS and silica interactions, it is also of value to examine the difference between BIMS and BIMS/silica by  $^{13}\text{C}$  solid state NMR measurements. Figure 22 shows the  $^{13}\text{C}$  solid state NMR spectra of these two materials. Assignments of some important peaks are shown. Similar structural features are observed in both spectra, thus indicating no chemical reactions between BIMS and silica.

However, it is recognized that there are 35 BrPMS groups in one BIMS 90–10 chain based on a calcula-

tion from the values of  $M_n$  and mol % BrPMS of the polymer. The interaction of only one BrPMS group with one  $\equiv\text{Si}-\text{OH}$  group on silica will render this chain bound to the silica. Solid state NMR may not have enough sensitivity to detect this interaction. Therefore, a model compound representing BIMS is more useful to study BIMS chemistry. For this reason, the following reaction of PIPBB and silica was carried out to simulate the Brabender mixing of BIMS with 50 phr silica. An identical amount of silica, and an amount of PIPBB that corresponds to the same molar

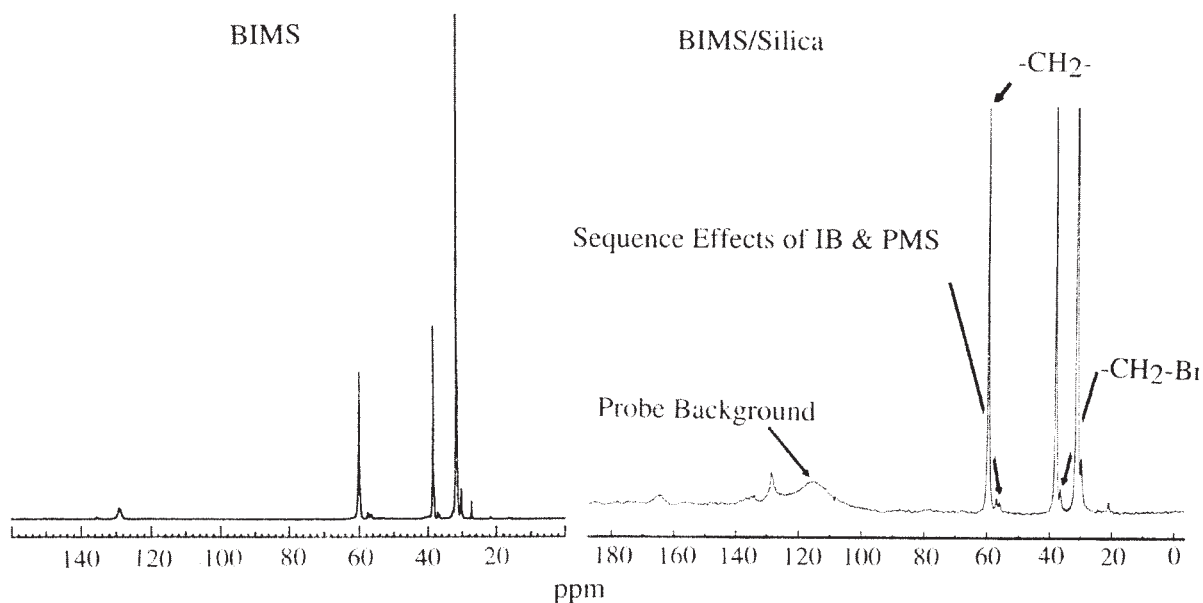
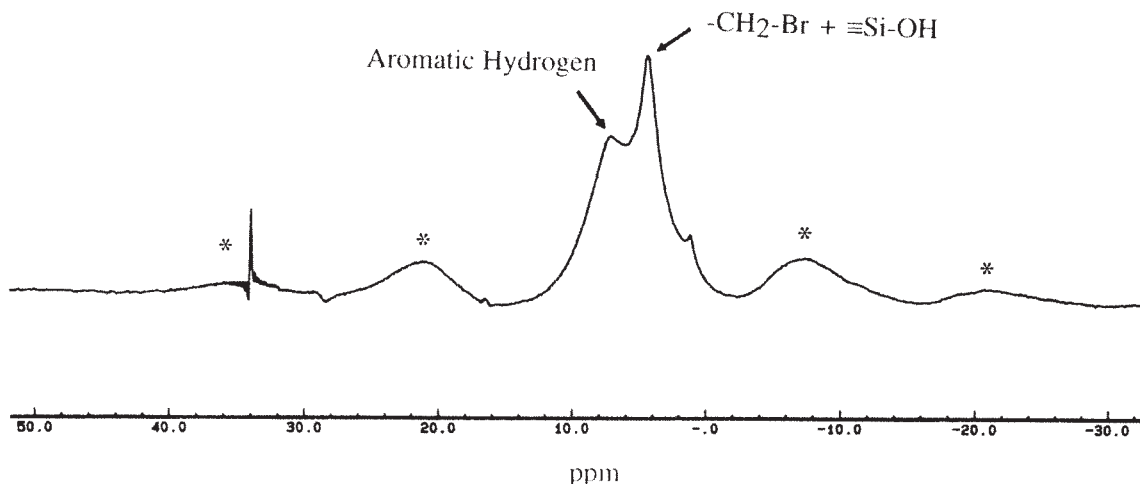


Figure 22 Some structural features are observed in the  $^{13}\text{C}$  solid state NMR spectra of BIMS and BIMS/silica. IB denotes isobutylene.



**Figure 23** Although PIPBB is adsorbed on the silica, there is no detectable shifting in the peak associated with the BrPMS group in PIPBB.

quantity of BrPMS in BIMS were stirred in refluxing 2,2,4-trimethylpentane (bp = 98°C; used to simulate the isobutylene portion of BIMS) for 15 min. The 2,2,4-trimethylpentane was then evaporated away. The PIPBB-treated silica was washed thoroughly eight times with chloroform. The  $^1\text{H}$  solid state NMR experiment of this washed PIPBB-treated silica was performed. The spectrum is shown in Figure 23, where the asterisks denote spinning side bands that arise from the chemical shift anisotropy of aromatic hydrogens. This indicates that PIPBB is strongly adsorbed on the silica, resulting in reduced molecular mobility. However, there is no detectable shifting in the peak at  $\sim 4.4$  ppm, suggesting again that there is no chemical bonding between BrPMS and  $\equiv\text{Si}-\text{OH}$ .

At this point, we have evidence both for and against the existence of strong bonding between BIMS molecules and the silica. The high bound rubber between them may be attributed to the following four occurrences:

1. There may be some chemical reactions between BIMS and silica.
2. Silica may catalyze crosslinking within BIMS.
3. Once the BIMS chain is adsorbed between the silicas with small interparticle spacings, it is more difficult to “debond” the chain from the adsorbing filler surface. Two adsorbed chains may entangle to form a trapped entanglement.
4. Mutually interactive agglomerates of silica via hydrogen bonding may resist dissolution of the adsorbed BIMS chains in cyclohexane or toluene (values of  $R_B$  for BIMS 90–10/silica at 25, 80, and 110°C are 75, 61, and 58%, respectively).

Occurrence (1) is ruled out based on the NMR results in Figures 19–23. A capillary rheometer, which measures the steady flow of BIMS and BIMS/silica at

115°C, has been used to check the validity of Occurrence (2). Results are shown in Table VIII. Only a moderate increase in viscosity of BIMS/silica relative to BIMS is observed, suggesting that Occurrence (2) is not valid. Up to this point, the high bound rubber in BIMS/silica is due to both or either one of the Occurrences (3) and (4), which represent physical adsorption and trapping of BIMS chains in silica. In summary then, it appears that there is no chemical bonding between BIMS molecules and silica.

## CONCLUSIONS

We summarize below some of our current understanding in BIMS/filler interactions:

- Bound rubber, viscoelastic, and stress–strain measurements can be used to study BIMS/filler interactions. A stronger polymer/filler interaction is characterized by a higher bound rubber, a broader loss modulus peak, and a higher yield stress of the BIMS/filler blend. Also, a larger specific surface area of the filler improves polymer/filler interactions.
- Heat treatment of the BIMS/CB blend results in a stronger polymer/filler interaction, the effect being more pronounced for the larger surface-area black.

**TABLE VIII**  
Capillary Flow<sup>a</sup> of Polymers

	Shear rate ( $\text{s}^{-1}$ )			
	5	10	$10^2$	$10^3$
BIMS 90–10	39	18	2.5	0.3
BIMS 90–10/Silica	50	25	3.5	0.7

<sup>a</sup> The values given represent shear viscosities (kPa s).

- The flow of the BIMS/CB blends under a tensile force can be analyzed by Eyring's model. The larger the CB surface area, the smaller is the activation volume per jumping segment of the BIMS elastomer and the higher is the activation energy of flow.
- Solid state NMR measurements on the BIMS/silica blend and on the BIMS model compound/silica blend (PIPBB/silica) provide no evidence of chemical bonding between the BrPMS groups in BIMS and the  $\equiv\text{Si}-\text{OH}$  groups on silica.

I wish to acknowledge K. O. McElrath for providing the polymer/filler blends, S. Shin for experimental assistance, and J. L. White for solid state NMR measurements.

### References

1. Yurekli, Y.; Krishnamoorti, R.; Tse, M. F.; McElrath, K. O.; Tsou, A. H.; Wang, H.-C. *J Polym Sci: Polym Phys Ed* 2001, 39, 256.
2. Tse, M. F.; Tsou, A. H.; Lyon, M. K. *Rubber World* 2003, 228, 30.
3. Wong, W. K.; Ourieva, G.; Tse, M. F.; Wang, H.-C. *Macromol Symp* 2003, 194, 175.
4. Barbin, W. W.; Rodgers, M. B. In *Science and Technology of Rubber*, 2nd ed.; Mark, J. E.; Erman, B.; Eirich, F. R., Eds.; Academic Press: New York, 1994; Chapter 9.
5. PPG catalog 1670D 1M 1092, PPG Industrial Inc., One PPG Place, Pittsburgh, PA 15272.
6. Bielski, R.; Frechet, J. M. J.; Fusco, J. V.; Powers, K. W.; Wang, H.-C. *J Polym Sci: Polym Chem Ed* 1993, 31, 755.
7. Baker, J. W.; Nathan, W. S. *J Chem Soc* 1980, 1935, 1844.
8. Crowley, J. I.; Rapoport, H. *J Org Chem* 1980, 45, 3215.
9. Nielsen, L. E. *Mechanical Properties of Polymers and Composites*; Marcel Dekker: New York, 1974; Vol. 1, p 155.
10. Ferry, J. D. *Viscoelastic Properties of Polymers*, 3rd ed.; John Wiley & Sons: New York, 1980.
11. Gessler, A. M. *Rubber Age* 1953, 74, 59.
12. Barton, B. C.; Smallwood, H. M.; Ganzhorn, G. H. *J Polym Sci* 1954, 13, 487.
13. Rehner, J., Jr.; Gessler, A. M. *Rubber Age* 1954, 74, 561.